Heliyon 9 (2023) e15686

Contents lists available at ScienceDirect

Heliyon

journal homepage: www.cell.com/heliyon

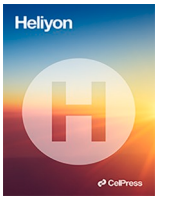

Research article

Elucidating the role of c-di-AMP in *Mycobacterium smegmatis*: Phenotypic characterization and functional analysis

Vikas Chaudhary, Aditya Kumar Pal, Mamta Singla, Anirban Ghosh *

Molecular Biophysics Unit, Indian Institute of Science, Bangalore, 560012, India

ARTICLE INFO

Keywords:
Mycobacterium smegmatis
Second messenger
c-di-AMP
Stress response
Antibiotics
Phenotypic microarray
RNA-Seq

ABSTRACT

Cyclic-di-AMP (c-di-AMP) is an important secondary messenger molecule that plays a critical role in monitoring several important cellular processes, especially in several Gram-positive bacteria. In this study, we seek to unravel the physiological significance of the molecule c-di-AMP in *Mycobacterium smegmatis* under different conditions, using strains with altered c-di-AMP levels: c-di-AMP null mutant (Δ*disA*) and a c-di-AMP over-expression mutant (Δ*pde*). Our thorough analysis of the mutants revealed that the intracellular concentration of c-di-AMP could determine many basic phenotypes such as colony architecture, cell shape, cell size, membrane permeability etc. Additionally, it was shown to play a significant role in multiple stress adaptation pathways in the case of different DNA and membrane stresses. Our study also revealed how the biofilm phenotypes of *M. smegmatis* cells are altered with high intracellular c-di-AMP concentration. Next, we checked how c-di-AMP contributes to antibiotic resistance or susceptibility characteristics of *M. smegmatis*, which was followed by a detailed transcriptome profile analysis to reveal key genes and pathways such as translation, arginine biosynthesis, cell wall and plasma membrane are regulated by c-di-AMP in mycobacteria.

1. Introduction

Bacterial second messengers have been shown to modulate diverse cellular functions in different bacteria; notified examples of such messengers include (p)ppGpp, c-di-GMP, and relatively new signaling molecule c-di-AMP [1,2]. The mere presence of different, yet structurally related molecules makes everybody curious to know the regulatory and functional basis of these messenger molecules under normal growth conditions and more importantly during stress adaptation. So far, c-di-AMP's role in many Gram-positive bacteria physiology is partially known which ranges from K^+ transport, DNA repair, cell wall metabolism, osmotic balance maintenance, antibiotic resistance, virulence, etc. [3–7]. In some cases, it is also shown to be involved in inducing the type I interferon response in mammalian hosts [8,9]. Decade-long research on c-di-AMP in mycobacteria has generated limited information [10–15] regarding the specific physiological functions of c-di-AMP and underlying mechanisms, which has entailed a thorough investigation of the role of c-di-AMP in *Mycobacterium smegmatis*, with and without any external stresses. In *M. smegmatis*, c-di-AMP is synthesized from condensation of two ATP molecules by enzyme DNA integrity scanning protein A (DisA) and degraded by enzyme Phosphodiesterase (Pde) into pApA. Though it was already known that the c-di-AMP level is constitutively maintained across all growth phases at a

Abbreviations: c-di-AMP, Cyclic di-adenosine monophosphate; DisA, DNA integrating scanning protein A; Pde, Phosphodiesterase; CFU, Colony forming unit; WT, Wild-type; MIC, Minimum inhibitory concentration; PM, Phenotypic microarray; RNA-seq, Ribonucleic acid-sequencing.

* Corresponding author.
E-mail address: ganirban@iisc.ac.in (A. Ghosh).

https://doi.org/10.1016/j.heliyon.2023.e15686
Received 20 May 2022; Received in revised form 17 April 2023; Accepted 18 April 2023
Available online 29 April 2023

minimum concentration [10] and some basic phenotypes related to c-di-AMP in *M. smegmatis* was learned, further understanding regarding how the complete lack and especially the overproduction of the c-di-AMP messenger affecting stress tolerance, antibiotic sensitivity and biofilm phenotype was needed to be studied in a comprehensive and interlinked manner. We found that modulating intracellular concentrations of c-di-AMP could alter a few basic phenotypes such as cell size, cell shape, colony morphology, as well as, some surface-related properties including cellular aggregation, sliding motility, and Biofilm/Pellicle formation. Our Phenotypic Microarray (PM) data indicated differential drug susceptibility/resistance profile of the mutant strains compared to Wild-type (WT), which involves antibiotics from all major classes; these observations were subsequently confirmed by Disc inhibition and Minimum Inhibitory Concentration (MIC) assay. Further, a genome-wide transcriptome analysis (by RNA-seq) of the mutants indicated few possible cellular mechanisms behind distinctive antibiotic responses and it also highlighted critical metabolic functions and cellular pathways regulated by c-di-AMP *in vivo*.

2. Materials and methods

2.1. Bacterial strains, media and growth conditions

A list of all the strains and plasmids used for this study is provided in Table S2 in the supplemental material. *M. smegmatis* MC^2155 (WT) and its knockout variants Δ*disA and* Δ*pde* (targeted gene deletion mutants); and their respective complemented strains (Δ*disA* + pDisA) & (Δ*pde* + pPde) were grown in Middlebrook 7H9 broth (MB7H9; Difco) with 2% (w/v) glucose as a carbon source and 0.05% (vol/vol) Tween 80 at 37 °C. The antibiotics kanamycin and hygromycin were used at a concentration of 25 μg/ml and 50 μg/ml respectively.

2.2. Construction of M. smegmatis deletion mutants

To understand the role of c-di-AMP in the physiology of *M. smegmatis*, *disA* and *pde* genes were deleted by the allelic exchange as described previously [16,17]. A recombination cassette was constructed on a plasmid pPR27 to delete open reading frames of *disA* and *pde* genes individually and the suicidal vector was transformed into competent *M. smegmatis* WT cells. The sucrose-resistant, gentamicin-sensitive, and kanamycin-resistant colonies were selected at 39 °C for further analysis. Disruption of the gene and the recombination event were verified by PCR (showing an increase in band size due to the insertion of kanamycin cassette) using genomic DNA as a template, followed by sequencing.

2.3. Complementation of $\Delta disA_{Msm}$ and Δpde_{Msm}

Functional copies of disA and pde genes were amplified from *M. smegmatis* MC^2155 genomic DNA as a template using primers. The amplicon was digested with restriction enzymes (Table S3) and cloned into the *E. coli*-mycobacterium shuttle vector pMV361, pre-digested with the same enzymes. The final constructs pMV361_*disA* and pMV361_*pde* were electroporated in Δ*disA* and Δ*pde strain respectively and screened on hygromycin 7H9 agar plate supplemented with* 2% glucose and 0.05% Tween.

2.4. Construction of disA point mutants by site-directed mutagenesis

The site-directed mutagenesis (SDM) technique was performed to generate different point mutants of *disA* using a standard procedure [18]. The PCR products containing the required nucleotide substitution were transformed into *E.coli* DH5α and the resulting plasmid containing the desired missense mutation was confirmed by sequencing. The final construct pMV261-*disA*(D84A) and pMV261-*disA* (R353A, R356A) were used as templates to amplify respective *disA* mutant alleles and subcloned in mycobacterium shuttle integrative vector pMV361 enzymes using same restriction enzymes and electroporated in Δ*disA* strain and screened on hygromycin 7H9 plate supplemented with 2% glucose and 0.05% Tween. All the primers used to make deletion mutants and plasmid constructs are listed in Table S3.

2.5. Estimation of colony architecture and morphology

As described earlier [19], 20 μl of the early stationary phase grown culture of *M. smegmatis* was spotted in the middle of the MB7H9 agar plates supplemented with 2% glucose and incubated at 37 °C for 8–12 days. Post incubation, images of the individual colonies were taken. For colony morphology, mid-log phase cultures were diluted 1:1000 and spotted 4 μL on MB7H9 agar plates supplemented with 2% glucose and incubated at 37 °C for 3 days. Post incubation, images of the individual colonies were taken.

2.6. Transmission electron microscopy

Transmission electron microscopy was carried out by adapting the protocol from Ghosh et al. [20]. Mid-log-phase *M. smegmatis* cultures were washed with PBST (Phosphate-buffered saline tween) twice and then 3 μl of the washed culture was drop cast on carbon-coated copper grids (Tedpella) and let stand for 10 min at room temperature. The sample containing the grid was blot dried using the Whatman filter paper and was negatively stained using 0.5% of uranyl acetate solution, then allowed to air dry. Then the stained grids were imaged with Talos L120C transmission electron microscope (Thermo Fisher) operated with 120 kV at room

temperature.

2.7. Scanning electron microscopy

The procedure of scanning electron microscopy was adapted from a previously published study [21]. Mid-log-phase *M. smegmatis* cultures were fixed with 2% glutaraldehyde for 30 min at room temperature and then stored at 4 °C for 4 h. After that, cells were washed with Phosphate buffer (0.1 M, pH-7.4) 3 times and resuspended in the same buffer. Samples were dehydrated through ethanol series 30%, 50%, 70%, 90% and 100% at 4 °C. A thin film of the sample was applied on a coverslip, air-dried for 20 min followed by sputter coating with gold particles; and observed under Zeiss Merlin VP FESEM with SE2 detector.

2.8. Biofilm formation assay

As described before [22], biofilms were grown in the Sauton's fluid base medium supplemented with 2% glucose as a carbon source. 1.5 ml. of the media was poured into each well of a 24-well plate and 1.5 μl of the washed (twice) stationary phase cells were added into each well and the plate was incubated at 37 °C in a humidified incubator for 4 days and the images were recorded under white light in a set of 3 biological replicates.

2.9. Sliding motility assay

The sliding motility assay was adapted from Martinez et al. [23]. Briefly, the cells were grown till OD_{600} 1.2 and then diluted to OD_{600} 0.4 in PBST buffer. 3 μl of the diluted cultures were spotted in the middle of MB7H9 plates solidified with 0.3% agarose without any carbon source. The plates were incubated at 37 °C for 2–3 days in a humidified incubator. Motility was measured by the diameter of the halo growth.

2.10. Cellular aggregation assay

The cellular aggregation assay was adapted from Deshayes et al. [24]. Briefly, early stationary phase cells were centrifuged at 10, 000 g for 1 min. CFU spotting was done with both supernatant and pellet. The aggregation percentage was calculated by using the CFU values from the supernatant and pellet fractions.

2.11. Ethidium bromide influx assay

The influx assay was adapted from Zhang et al. [25]. Briefly, *M. smegmatis* cultures were grown at 37 °C in MB7H9 medium to an OD_{600} of 0.9–1. Cells were washed twice with phosphate buffer saline (PBS) with 0.05% tween80, then resuspended in 1/3rd volume of the same buffer and kept at 37 °C shaking for 1 h to induce starvation. After that, carbonyl cyanide m-chlorophenylhydrazone (100 μM) was added (which acts as an efflux pump inhibitor) and cells were further incubated for 30 min in the same condition. Next, Ethidium bromide (0.5 μg/ml final concentration) was added and cells were immediately taken into 96 well black plates. To quantify the accumulation of Ethidium bromide (EtBr), fluorescence was checked for the next 1 h (with a 5-min interval between two readings) in Varioskan Flash multimode reader (Thermo Fisher Scientific) at 530 nm and 590 nm wavelength for excitation and emission respectively.

2.12. Pellicle formation assay

As described previously [26], stationary-phase cultures of the strains were diluted to an $OD_{600}$of 0.03 in LB media and kept standing for at 37 °C without any disturbances and then imaged after 5 days.

2.13. Stress tolerance assays

M. smegmatis strains were grown until the mid-log phase and then normalized to OD_{600} 0.7. The bacteria were diluted by 10-fold serial dilutions and 4 μl of cells from each dilution were spotted in MB7H9 agar medium. After the drying of the spots, the plate was exposed to UV irradiation (0.15 mJ/cm^2) [27] and then incubated at 37 °C for 3 days in the dark. For SDS treatment, OD_{600} 0.7 cells were exposed to 0.05% SDS (final concentration) for 4 h and then spotted on MB 7H10 agar plates. During MMS treatment, mid-log phase cultures were centrifuged and resuspended in an equal volume of PBST (Phosphate buffer saline + tween) and treated with 0.5% MMS (final concentration) for 20 min at 24 °C then spotted (10-fold serial dilution) on MB 7H10 agar plates [11]. Survival percentage was calculated as the percentage of CFU remaining after exposure to the respective stresses compared to the CFU in an untreated condition.

2.14. Phenotypic microarray analysis

A phenotypic microarray (PM)assay was performed using the protocol of Gupta et al. [22]. In brief, the transmittance of the logarithmic phase bacterial cultures were adjusted to 81% and tetrazolium violet was added to a final concentration of 0.01%. 100 μl of

the cultures were inoculated into the wells of PM plates 1 to 20 coated with chemicals/antibiotics and kept in the Omnilog incubator (BiOLOG^{TM}) at 37 °C for 4 days. The dye reduction values were converted to the area under the curve (AUC) by using the parametric software module of Biolog-Omnilog software. The AUCs for the strains were compared and overlaid as the test strain versus reference strain AUC.

2.15. MIC (Resazurin Microtiter Assay Plate, REMA) assay

MIC values were estimated using REMA adapted from an earlier protocol [28]. In brief, the transmittance of the culture was adjusted to a McFarland turbidity standard of 1 and then diluted to 1:10. Next, 196 μl portions of the diluted culture were inoculated into 96 well microtiter plates containing a 2-fold serial dilution of the antibiotics (4 μl). Plates were sealed and incubated at 37 °C. After 36 h, 30 μl of 0.01% resazurin dye was added to each well, and plates were further incubated for 4–6 h. The color of the resazurin changed from blue to pink due to bacterial growth. The MIC was determined as the minimum antibiotic concentration at which the resazurin dye did not change color.

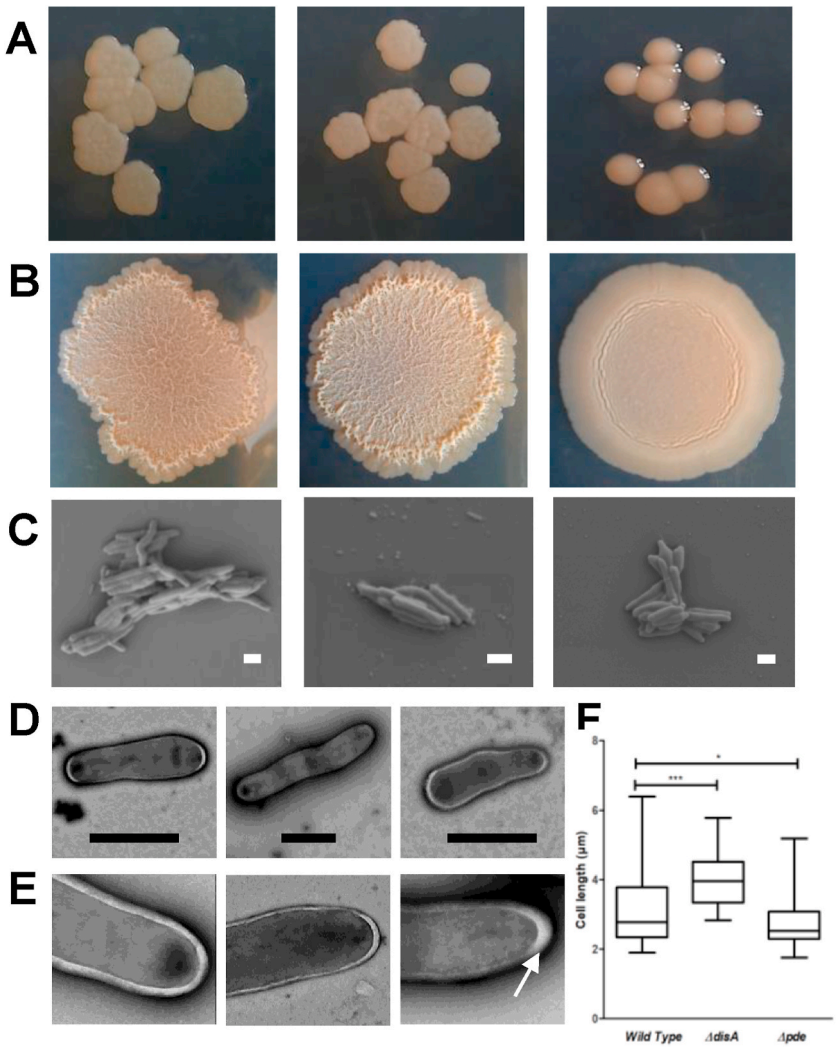

Fig. 1. Modulating intracellular c-di-AMP concentration affects the colony characteristics of *M. smegmatis* WT (left panel), *M. smegmatis* Δ*disA* (middle panel) and *M. smegmatis* Δ*pde* (right panel): **(A)** Colony size and morphology (B) Colony architecture. Individual cell shape and size determination was done by electron Microscopy. Representative microscopic images of *M. smegmatis* WT (left panel), *M. smegmatis* Δ*disA* (middle panels) and *M. smegmatis* Δ*pde* (right panels), with Scanning Electron Microscopy (SEM) (C) and Transmission Electron Microscopy (TEM) (D) microscopy (scale bars = 2 μm) reveals the difference in cell morphology linked to intracellular c-di-AMP concentration. (E) Closer inspection of some TEM images reveals occasional increased outer layer thickness at poles in *M. smegmatis* Δ*pde* strains, highlighted by white arrow; (F) Cell length distribution analysis of individual strains. Lengths of at least 50 cells of each strain from different electron micrographs are measured and plotted using the box plot analysis function from GraphPad Prism 5. The whiskers in the plot represent minimum and maximum values. The mean lengths are found to be 3.11 μm for the WT, 3.98 μm for the *M. smegmatis* Δ*disA* and 2.70 μm for the *M. smegmatis* Δ*pde* strain.

2.16. Disc diffusion assay

As previously described [29], *M. smegmatis* strains were grown until the mid-log phase and 100 μl of the OD_{600} 0.7 cultures were spread on MB 7H10 agar plates and left for drying. After that, discs soaked with 10 μl of erythromycin (50 mg/ml) and ciprofloxacin (2.5 mg/ml) stocks were aseptically kept in the middle of the plate using a sterile tweezer. Plates were further incubated at 37 °C for 3 days and the zone of inhibition (cm^2) was calculated as a measurement of antibiotic sensitivity.

2.17. Transcriptome analysis by RNA-Seq

As described earlier [30], *M. smegmatis* cells were grown till the early exponential phase (OD_{600}~0.6), washed twice with PBS and dissolved in RNA later solution with TRIzol (Invitrogen) and placed on ice. Subsequent steps of RNA extraction, DNA synthesis, library preparation, and alignment were carried out at Clevergene biocorp private limited, Bangalore, India. Briefly, the cells were mechanically disrupted by bead beating and the supernatant was collected for RNA extraction using HiMedia HiPurA extraction kit and finally eluted with 15 μl of RNase free water. The RNA quality assessment was done using RNA HS ScreenTape System (Catalog: 5067–5579, Agilent) and the RNA concentration was determined on Qubit® 3.0 Fluorometer (Catalog: Q33216, Thermo Fisher Scientific) using the Qubit™ RNA HS Assay Kit (Catalog: Q32855, Thermo Fisher Scientific). Next, 500 ng of total RNA was taken for rRNA depletion using QIAseq FastSelect −5S/16S/23S Kit (Catalog: 335925, Invitrogen) according to the manufacturer's protocol. NEB Next Ultra II RNA Library Prep Kit (Catalog: Catalog: E7775S, New England Biolabs) for Illumina was used for the library preparation. The enriched transcriptome was chemically fragmented in a magnesium-based buffer at 94 °C for 10 min. The fragmented samples were primed with random hexamers, and reverse transcribed to form cDNA and the first-strand cDNA reactions were converted to dsDNA. Furthermore, the DNA was amplified by 12 cycles of PCR with the addition of NEB Next Ultra II Q5 master mix, and "NEB Next® Multiplex Oligos for Illumina" to facilitate multiplexing while sequencing. After the library quantification and validation, the sequence data were generated using Illumina HiSeq. After removing adapter sequences and low-quality bases, the processed reads were mapped on the reference genome *Mycolicibacterium smegmatis* MC^2155 (NCBI Genbank accession NC_008596) for further analysis of differential expression, gene ontology and pathway enrichment.

3. Results

3.1. Modulating intracellular c-di-AMP concentration affects basic phenotypes

To directly study the role of c-di-AMP in *M. smegmatis* basic physiology, we used two deletion mutants*: M. smegmatis* Δ*disA* and *M. smegmatis* Δ*pde*, which corresponds to c-di-AMP null mutant and over-expressing mutant strains respectively. As a part of strain validation, apart from PCR (Fig. S1) and sequencing confirmation assuring respective gene deletions, we measured the c-di-AMP level in both the deletion mutants along with WT *M. smegmatis* by mass spectrometry. After checking the peak identity at *m/z* of 659 using standard c-di-AMP**,** we confirmed the lack and abundance of the c-di-AMP molecule in respective mutant strains (Fig. S2). Once the strains were verified, we constructed individual complementation strains by cloning *disA* and *pde* genes in a single copy integrating vector pMV361 and transforming them into the corresponding knockout strains resulting in the construction of complementation strains. With these 5 strains, we first checked how the basic phenotypes have been affected by unbalancing the steady-state homeostasis of c-di-AMP messenger, which is hypothesized to be the key factor during normal growth and stress tolerance.

First, we began our study by checking a few basic cellular phenotypes (without any stress) which were partly known [10,12] and our primary observation inferred minute growth deficiency in *M. smegmatis* Δ*pde* strains in broth cultures and agar plates. Precisely, *M. smegmatis* Δ*pde* strain had a minor growth defect in the exponential phase in MB7H9 media (Fig. S3) and formed smaller colonies with different morphology on agar plates (Fig. 1A). These observations were in line with previous studies where plasmid-based ectopic overexpression of *disA* (pMV261-*disA*) was carried out in *M. smegmatis* [10,31]. Consequently, when we tested *M. smegmatis* Δ*pde* + pMV361-*pde*, we could not observe any growth defects highlighting the direct role of high intracellular concentration of c-di-AMP, and not immoderate DisA-DNA interaction behind the phenotype. However, *M. smegmatis* Δ*disA* strain did not show any growth deficiency (Fig. S3) compared to WT further implying the significance of maintaining a low concentration of c-di-AMP inside cells. Similar observations with smaller colony size in a high c-di-AMP-producing strain have been reported previously with overexpression constructs [10]**.**

Next, we found that the colony architecture was drastically changed in the c-di-AMP overproducing strain *M. smegmatis* Δ*pde* compared to WT, and the phenotype was reversed in the respective complementation strain (Fig. S4). The colony surface became smooth, uniform, and glossy in the *M. smegmatis* Δ*pde* strain (Fig. 1B), which is possibly linked with major changes in surface properties. On the other hand, all the other strains formed characteristic *M. smegmatis* rough and dry colonies (Fig. 1B, Fig. S4).

Once we were certain that some of the basic phenotypes were consequentially altered, we were interested in changes in individual cell shape and size of WT and mutants. First, we did Scanning Electron Microscopy (SEM) to reveal differences in 3D cell morphology and surface properties and found that cell length was marginally increased in the case of *M. smegmatis* Δ*disA* strain compared to WT, whereas in a high c-di-AMP strain (Δ*pde)* cells have become shorter and thicker (Fig. 1C). Previously it has been reported also that altering the concentration of another second messenger such as (p)ppGpp could have an impact on *M. smegmatis* cell elongation [32]. Further analysis with Transmission Electron Microscopy (TEM) also suggested that *M. smegmatis* Δ*disA* cells were longer (Fig. 1D) and possess almost uniform cell width and slightly reduced outer layer thickness compared to WT cells. On the other hand, *M. smegmatis* Δ*pde* cellular width is variable and often shown to have a thicker outer layer, especially in the poles (Fig. 1E). Finally, we measured the

individual cell lengths of different strains from the TEM image dataset, and the comparison revealed significant cell length variation across strains as a function of c-di-AMP concentration (Fig. 1F). Though significant differences in terms of cell length, shape, and outer layer thickness were observed linked to varying c-di-AMP concentrations, the exact pathway/mechanism needs to be studied in the future.

3.2. Surface properties are significantly altered in high c-di-AMP strain

Visible differences in the colony architecture of *M. smegmatis* Δ*pde* strain demanded a further investigation of other cell surface properties. Hence, we quantified the level of cellular aggregation by a previously described protocol [22] and found that the intracellular c-di-AMP concentration was directly correlated with the aggregation level of cells, where *M. smegmatis* Δ*pde* tends to form more cellular aggregates and *M. smegmatis* Δ*disA* strain formed lesser aggregate compared to WT. As expected, both *disA* and *pde* complemented strains behaved like a WT(Fig. 2A).

Next, we checked the surface hydrophobicity as a function of glycopeptidolipids (GPL) of individual strains in terms of sliding motility on agarose plates using a previously described method. Here we found that *M. smegmatis* Δ*disA* strain was visibly more motile (quantification of motility was estimated by measuring the spreading radius from the center point in an agarose petriplate where the inoculation was done) than WT, on the other hand, *M. smegmatis* Δ*pde* strain had significantly lost motility compared to WT (Fig. 2B). A

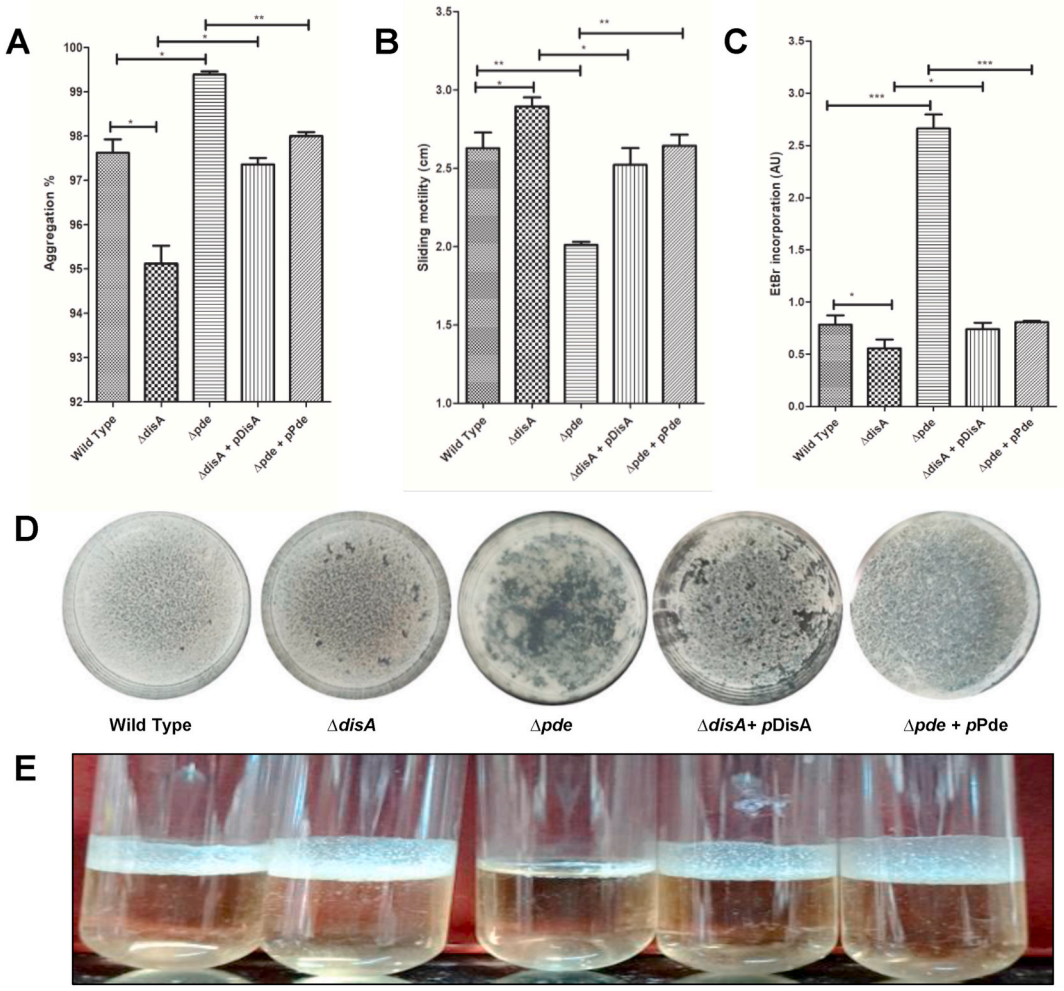

Fig. 2. Estimation of cell surface-associated Phenotypes by comparison of (A) Cellular aggregation profile (%), (B) Sliding motility (in cm.) and (C) EtBr incorporation (AU) in *M. smegmatis* WT, Δ*disA,* Δ*pde* and the respective complementation strains. Error bars indicate the standard deviations from three independent experiments. (D) Biofilm formation phenotypes shows that *M. smegmatis* WT and *M. smegmatis* Δ*disA* form a thick biofilm in 24 well plates at 37° after 4 days, whereas *M. smegmatis* Δ*pde* strain is defective in biofilm formation, but the phenotype is restored in the complementation strain. (E) Pellicle formation is estimated at the air-liquid interface of the standing LB cultures of different strains and *M. smegmatis* Δ*pde* strain was found to be significantly compromised in forming a pellicle. The graphs are plotted using GraphPad Prism 5. *** = $P < 0.001$; ** = $P < 0.01$; * = $P < 0.05$.

major change in cellular aggregation and sliding motility was also reported before using *M. smegmatis* + pMV261-*disA* strain, but that could be an indirect effect of a severe growth deficiency of the strain reported in the same study [31]. Moreover, just by overexpressing DisA (a dual-function protein), it was not clear if the observed phenotype was due to high c-di-AMP concentration or increased DisA-DNA interaction. In our study, we showed *pde* complementation strain's aggregation profile and sliding motility pattern remain unchanged like WT (Fig. S5), which further points towards a direct link between intracellular c-di-AMP concentration with aggregation and motile property of *M. smegmatis*. Often this change in surface motility has been linked to different glycopeptidolipids (GPL) fractions in the cell wall [33,34] and from this result, it is evident c-di-AMP could possibly play a role in cell wall structure and synthesis. As has been previously mentioned that c-di-AMP responsive transcriptional factor DarR is responsible for the regulation of fatty acid biosynthesis in *M. smegmatis* [12], the drastic change in surface properties could be due to the alteration of fatty acids composition in cell wall and membrane.

Our hypothesis regarding altered surface properties linked with envelope structure and porosity was explored by the Ethidium bromide (EtBr) influx assay. It was found that EtBr influx was almost 3 fold higher in *M. smegmatis* Δ*pde* strain from WT, whereas no

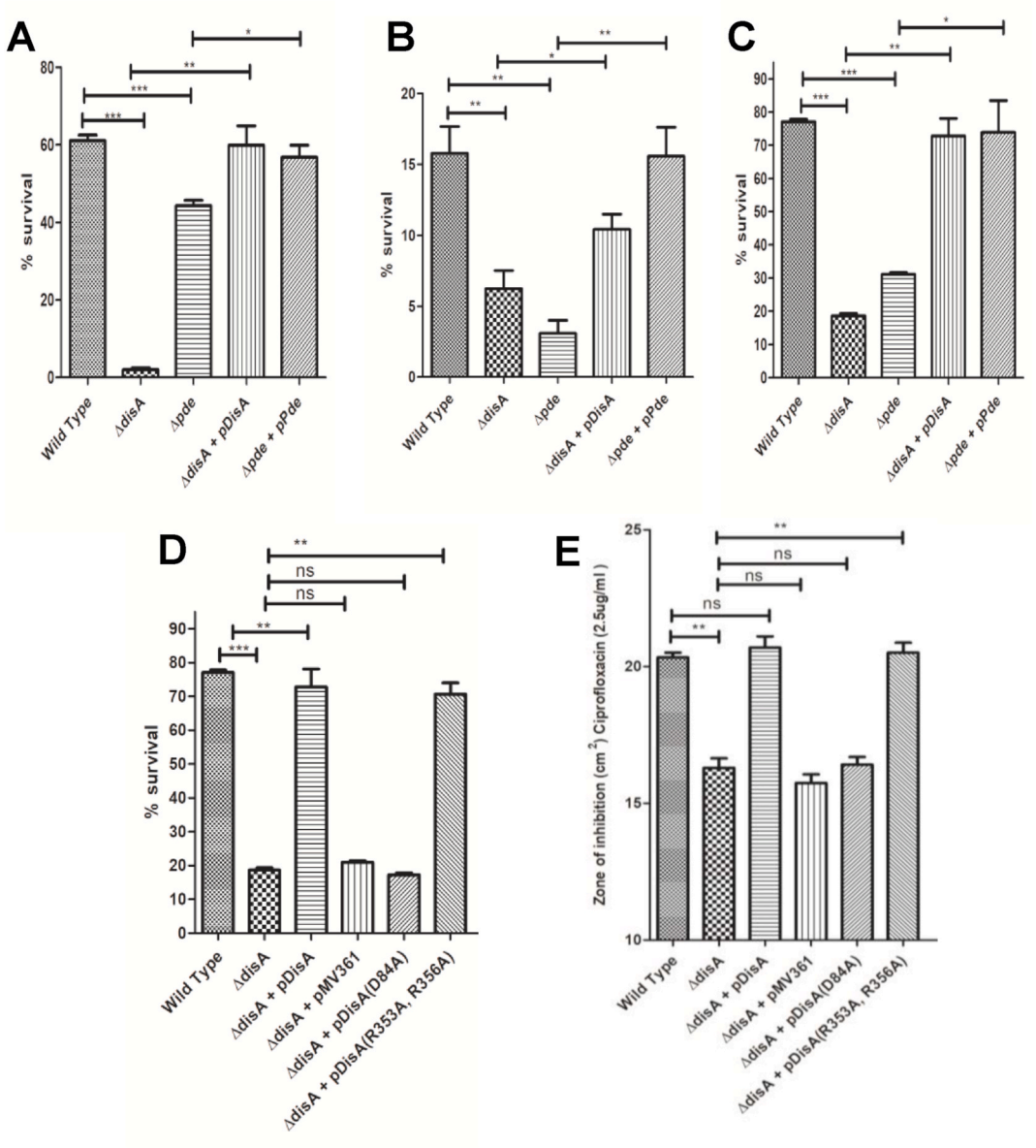

Fig. 3. Stress tolerance assays. *M. smegmatis* Δ*disA* & *M. smegmatis* Δ*pde* strains display sensitivity to several stresses. Percentage survival is calculated after 0.5% MMS treatment (A), 0.15 mJ/cm^2 UV irradiation (B) and 0.05% SDS treatment (C). DisA protein's multi-domain nature and interdomain functional independency are illustrated by SDS treatment (D) and disc diffusion assay predicting ciprofloxacin sensitivity (E). The graphs are plotted using GraphPad Prism 5. *** = $P < 0.001$; ** = $P < 0.01$; * = $P < 0.05$.

difference was observed with *M.smegmatis* Δ*disA* strain (Fig. 2C). Since this assay was done in presence of a well-known efflux pump inhibitor CCCP [35] at a non-toxic concentration, the differential uptake of EtBr highlighted the difference in membrane permeability or cell wall rigidity [5,36] or functional regulation of particular membrane transporters by c-di-AMP, which needs to be investigated in the future.

3.3. High c-di-AMP concentration inhibits biofilm formation in M.smegmatis

One of the well-studied phenotypes linked with second messengers such as (p)ppGpp and c-di-GMP is biofilm formation. We also wanted to study the possible link between c-di-AMP concentration and biofilm formation characteristics in *M. smegmatis*. Our data suggested that, though *M. smegmatis* Δ*disA* strain had no visible difference in biofilm formation in 24 well plates with *M. smegmatis* WT, *M. smegmatis* Δ*pde* possesses the inadequate ability to form and maintain biofilm in identical conditions (Fig. 2D). In mycobacteria, air-liquid interphase pellicle formation is also often considered a reliable marker for biofilm formation, and we found that *M. smegmatis* Δ*pde* strain was significantly compromised in forming pellicle when grown in glass tubes, whereas *M. smegmatis* Δ*disA* strain formed slightly more pellicle than WT (Fig. 2E). In both the direct and indirect assays to quantify biofilm formation, the high c-di-AMP strain showed a clear difference in biofilm formation further highlighting c-di-AMP's contribution in maintaining such complex phenotypes. Because there was hardly any difference between WT and Δ*disA* strain, it was clear that c-di-AMP's presence and absence do not control biofilm properties in *M. smegmatis*, rather the intracellular c-di-AMP concentration plays a critical role in rigid biofilm formation in *M. smegmatis* whereas a closely related second messenger c-di-GMP has proved to have a negligible impact [37]. Thus, any ectopic increase in c-di-AMP level severely affects the biofilm formation phenotype of *M. smegmatis* and possibly makes the cells more prone to external stresses, such as antibiotics. Hence from a bacterial cell's point of view, it is pivotal to keep the c-di-AMP level under check.

3.4. c-di-AMP is involved in several stress tolerance pathways

Previously it was reported that the *disA* gene in *M. smegmatis* exists in a multi-gene operon along with two other genes *radA* and *lpqE* [31]. The DisA and RadA proteins have been studied well and found to have a definite role in DNA damage response when cells encounter genotoxic stressesv [2,38,39]. Apart from being the sole DAC enzyme responsible for c-di-AMP synthesis, DisA functions as a DNA integrity scanning enzyme with a defined role in DNA repair and mutagenesis [38–40] in other bacteria. Based on a previous study, RadA and DisA are thought to be co-transcribed using the common promoter present upstream of the operon and claim that the RadA protein inhibits the synthetic activity of DisA by physically interacting with the DisA enzyme [31]. Similarly, two other studies of *B. subtilis* have shown how the DisA-mediated c-di-AMP synthesis was affected by interaction with RadA and Holliday Junction (HJ) DNA [41] and how DisA together with RadA works to circumvent replicative stress [39]. These results suggest DisA and RadA proteins are functionally linked and DisA-RadA interaction favors the DisA enzyme to exclusively participate in the DNA damage repair, while the c-di-AMP synthetic activity remained largely inhibited. Since c-di-AMP and DisA have been previously linked with DNA damage repair in different organisms including *M. smegmatis,* we first estimated the survival of the deletion mutant strains against several genotoxic stresses.

Our data reconfirmed the previous report [11] that *M. smegmatis* Δ*disA* strain is very sensitive (~30 fold) to 0.5% methyl methanesulfonate (MMS) treatment, which is known to methylate DNA bases and cause replication fork arrest. On the contrary, high c-di-AMP mutant *M. smegmatis* Δ*pde* showed a much smaller difference with WT (Fig. 3A), which could indicate that the DisA scanning enzyme, rather than the c-di-AMP molecule, is important to prevent MMS driven toxicity by an unexplored mechanism.

Next, we checked how the deletion mutants behaved under UV exposure (0.15 mJ/cm^2). We found that the *M. smegmatis* Δ*disA* strain is ~3–4 fold more sensitive than WT. To our surprise, we found that the *M. smegmatis* Δ*pde* strain was more sensitive to UV stress (~5–6 fold) compared to WT (Fig. 3B), which is possibly linked to impeded *recA* function [11]. The fact that both null- and overproducing-c-di-AMP mutants were sensitive to UV stress, apparently implied that both higher and lower concentration of c-di-AMP is detrimental for cells under such conditions.

Other than, DNA stresses we treated the mutants with ionic detergent Sodium dodecyl sulfate (SDS) and found that both *M. smegmatis* Δ*disA* and *M. smegmatis* Δ*pde* strains were found to be sensitive (20–30% survival) to 0.05% SDS compared to WT (Fig. 3C). Respective complementation strains showed a similar level of sensitivity (70–80% survival) with WT further suggesting how the varying concentration of c-di-AMP could make cells more prone to cell lysis possibly due to the membrane and cell wall protein denaturation (Fig. 3C).

Finally, as c-di-AMP has been previously studied [4,42] to contribute to ion homeostasis and envelope stress in several Gram-positive bacteria, we checked the c-di-AMP mutants strains' (*M. smegmatis* Δ*disA* and *M. smegmatis* Δ*pde)* response against osmotic stress (500 mM final concentration NaCl, sodium chloride and KCl, potassium chloride) and found no significant difference in the tolerance/survival levels when compared to *M. smegmatis* WT and Δ*disA* mutant, but Δ*pde* mutant showed a low level of sensitivity (data not shown).

3.5. Identifying DisA protein's multi-domain nature and mutational uncoupling of two activities

DisA being a multi-domain and dual-functional protein [2,31], we wanted to understand the specific role of different domains during stress tolerance by individually putting missense amino acid substitutions of the key residues either known or identified through bioinformatic modeling. DisA belongs to deadenylate cyclase (DAC) class of enzymes and comprises of an N-terminal DAC

domain that participates in the synthesis of c-di-AMP using ATP as substrate, followed by a domain linker and a DNA-binding helix-hairpin-helix (HhH) domain whose main function is to monitor DNA damage. As we found out, *M. smegmatis* Δ*disA* strain has shown clear sensitivity against SDS treatment and significantly resistant phenotype to ciprofloxacin compared to WT (described by Phenotypic Microarray and disc inhibition assay later) we complemented *M. smegmatis* Δ*disA* strain with different *disA* mutants (c-di-AMP synthesizing catalytic mutant and DNA binding mutant) in pMV361 integrative vector. In all our assays, *M. smegmatis* Δ*disA* + *p*DisA (WT copy) and *M. smegmatis* Δ*disA* + *p*Empty served as positive and negative controls respectively to check the reversal of phenotype for *M. smegmatis* Δ*disA* strain to WT upon complementation with different DisA point mutants (D84A:c-di-AMP synthesizing catalytic mutant [31]; R353A, R356A (putative DNA binding mutant). Upon SDS treatment it was found that *M. smegmatis* Δ*disA* + *p*DisA(D84A) behaved similarly to *M. smegmatis* Δ*disA* + *p*Empty and failed to reverse the SDS sensitivity, whereas *p*DisA(R353A, R356A) complementation construct was able to make the *M. smegmatis* Δ*disA* strain less sensitive to 0.05% SDS like *M. smegmatis* Δ*disA* + *p*DisA (WT copy) (Fig. 3D). Then, we checked whether the ciprofloxacin resistance phenotype was reversed with complementation of different DisA point mutants and it was found that, *M. smegmatis* Δ*disA* + *p*DisA (D84A) retained the resistance phenotype like *M. smegmatis* Δ*disA* strain and *M. smegmatis* Δ*disA* + *p*DisA (R353A,R356A) strain became sensitive to ciprofloxacin like WT and *M. smegmatis* Δ*disA* + *p*DisA (WT copy) complementation strain (Fig. 3E). Finally, we wanted to see the UV hypersensitivity of the Δ*disA* strain was due to a lack of c-d-AMP or DisA repair enzyme, we complemented the *M. smegmatis* Δ*disA* strain with different point mutants and found that *M. smegmatis* Δ*disA* + *p*DisA(D84A) complementation strain remained sensitive to UV irradiation like *M. smegmatis* Δ*disA* + *p*Empty strain, whereas *M. smegmatis* Δ*disA* + *p*DisA(R353A, R356A) could manage to survive better by ~2 fold (Fig. S6), but not to the same extent like WT *disA* complementation strain. These observations led us to ascertain the fact that SDS sensitivity and ciprofloxacin resistance phenotypes of *M. smegmatis* Δ*disA* strain are due to the lack of c-di-AMP and not due to loss of DisA enzyme's DNA scanning property. This mutational uncoupling study of the DisA protein by targeting single amino acid residues in either domain of the enzyme further corroborated the multi-domain characteristics and inter-domain functional independency of this important dual-function protein in *M. smegmatis*.

3.6. Phenotypic Microarray analysis revealed a direct link between c-di-AMP concentration and differential drug susceptibility

To gain a deeper understanding of how c-di-AMP concentration plays a critical role in drug resistance or sensitivity phenotypes in *M. smegmatis*, we performed the Phenotypic Microarray (PM) analysis which gave a vast platform to check antibiotic sensitivity/resistance phenomenon across various concentrations of 240 different antibiotics/chemicals in a high throughput manner [43]. The growth of the respective strain in presence of a particular compound was calculated based on dye reduction values plotted as a function of time up to 96 h. Whether the c-di-AMP null- and overproducing-mutants were growing better or worse than WT was deduced by PM Omnilog software (BiOLOG^{TM}), which could simultaneously compare the AUC (Area Under Curve) values of two strains for a specific antibiotic concentration (Fig. S7). By analyzing the significant differences in AUC values between *M. smegmatis* WT and Δ*pde* strain first, we shortlisted a few antibiotics (with different Mechanism of action) for which Δ*pde* strain showed hypersensitivity, as evidenced by lower AUC values. Next, we compared the AUC values of the same drug concentrations (specific well in the PM plate) between *M. smegmatis* WT and Δ*disA* strain to know if there was any similar or more importantly reverse trend was observed. Based on these considerations, our phenotypic microarray data showed that the *M. smegmatis* Δ*pde* strain was significantly sensitive to an array of

A

PM Plate wells	Drug name	Mode of action	Difference in AUC	
			Wt / Δ*disA*	Wt / Δ*pde*
Plate 20B, D7	Ciprofloxacin	DNA replication	2775	-7047
Plate 12B, H7	Rifampicin	Transcription	7702	-13199
Plate 11C, F05	Erythromycin	Translation	4252	-1640
Plate 12B, C7	Vancomycin	Cell wall	1099	-8519

B

Strain	MIC (μg/ml)			
	Ciprofloxacin	Rifampicin	Erythromycin	Vancomycin
Wild type	0.25	16	32	4
Δ*disA*	0.25	16	32	4
Δ*pde*	0.125	2	8	0.5
Δ*disA*+*p*DisA	0.25	16	32	4
Δ*pde*+*p*Pde	0.25	16	32	4

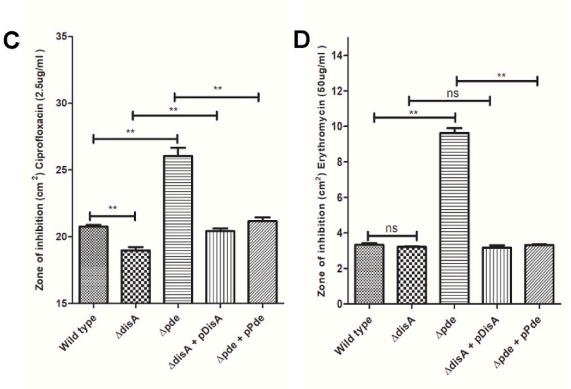

Fig. 4. Phenotypic microarray analysis in *M. smegmatis* WT, *M. smegmatis* Δ*disA* & *M. smegmatis* Δ*pde* strains. The strains were grown in 96-well plates in the presence of different antibiotics with tetrazolium violet as an indicator for growth. The change in the colour of the dye due to respiration was measured, and the absorbance is plotted as a function of time. (A) Comparison of growth profiles in terms of area under curve (AUC) values; (B) MIC values with representative antibiotics for the Wild-type *M. smegmatis* and its isogenic variants were determined using the REMA method. Disc inhibition assay in terms of zone of inhibition was calculated with ciprofloxacin (C) and erythromycin (D), revealing a high level of sensitivity *M. smegmatis* Δ*pde* strain, further confirming PM observation and elucidating the direct relationship between c-di-AMP concentration and differential drug susceptibility. *** = $P < 0.001$; ** = $P < 0.01$; * = $P < 0.05$.

antibiotics like ciprofloxacin, rifampicin, erythromycin, and vancomycin (Fig. 4A). Though the level of sensitivity differed between different antibiotics, this preliminary observation has thrown a light on how c-di-AMP concentration could imitate the multi-drug resistance or sensitivity phenotype of a strain, which was not reported before as per our knowledge. In the case of all 4 antibiotics, *M. smegmatis* Δ*disA* strain showed moderate/significantly higher AUC values compared to WT further corroborating essentiality for an optimum intracellular concentration of c-di-AMP. Next, we confirmed the PM observation of increased sensitivity of Δ*pde* strain in two ways: Minimum Inhibitory Concentration (MIC) assay and antibiotic disc diffusion assay, to assess the effect in both liquid and solid media. To be sure, the observed drug sensitivity was indeed due to the deletion of the *pde* gene, and not due to any secondary polar effect arising from the deletion of the gene we used complementation strain (*M. smegmatis* Δ*pde* + *p*Pde) in our MIC and disc diffusion assays. Both the complementation strain: Δ*pde* + *p*Pde and Δ*disA* + *p*DisA showed similar levels of resistance (MIC value and zone of inhibition) for all 4 antibiotics highlighting the direct relationship between varied c-di-AMP concentration and differential drug susceptibility, whereas *M. smegmatis* Δ*pde* strain was 2–8 fold more sensitive to all 4 antibiotics compared to WT strain (Fig. 4B). Similarly, *M. smegmatis* Δ*pde* strain produced a significantly bigger zone of inhibition in presence of 2.5 μg/ml ciprofloxacin (Fig. 4C) and 50 μg/ml erythromycin (Fig. 4D) discs and with the single copy complementation of the *pde* gene the sensitivity was reverted to the WT level. Though there is a common trend that high intracellular c-di-AMP concentration makes the cell more vulnerable to a different class of antibiotics, the specific molecular mechanism related to the individual mode of action of the drug remains to be investigated in the future. Table S1 contains the list of the top 40 antibiotics/chemicals in which the area under curve (AUC) difference between WT and respective mutants was shown to be the highest on either side (loss and gain).

3.7. RNA-seq based transcriptome analysis highlighted key pathways regulated by c-di-AMP

After we confirmed c-di-AMP's direct role in both stress adaptation and drug sensitivity, further insights into the transcriptional landscape were unraveled by comparing the global expression profiles of all the expressed genes. RNA-Seq technique was used to study alternative gene expression in *M. smegmatis* WT, Δ*disA,* and Δ*pde* strains [44]. Since c-di-AMP is known to be produced at a basal level under normal physiological conditions (Fig. S2), cells were grown till the mid-log phase, harvested to isolate intact RNA, and then performed the RNA-seq analysis. Differential expression analysis was carried out using the DESeq2 package and genes (more than a total of 5 reads) with absolute log2 fold change ≥ 1 with p-value ≤ 0.05 were significant. Out of a total of 6518 expressed genes for all strains, in *M. smegmatis* WT (reference) vs *M. smegmatis* Δ*disA* (test) comparison, the total number of significantly altered genes was found to be 327. Similarly, *M. smegmatis* WT (Reference) vs *M. smegmatis* Δ*pde* (Test) comparison revealed a total of 109 genes were differentially expressed (upregulated + downregulated) (Fig. 5A). The expression profile of the differentially expressed genes across the samples was presented in volcano plots (Fig. 5B). The genes that showed significant differential expressions (highlighted in the volcano plot with statistical significance) were used for Gene Ontology (GO) and pathway enrichment analysis. Next, we performed an

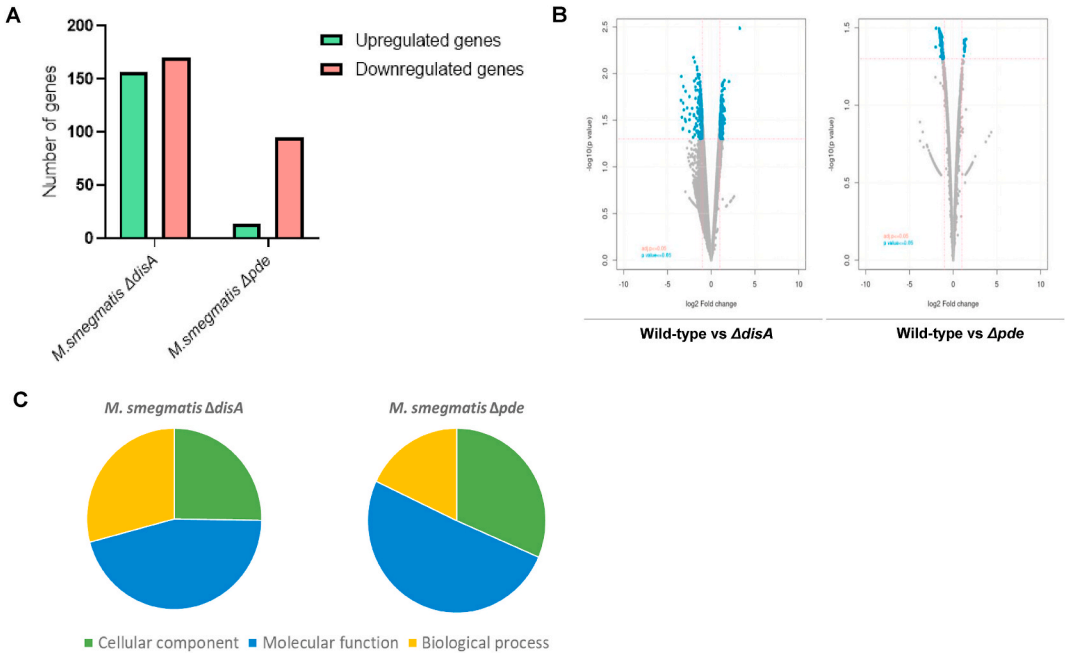

Fig. 5. Transcriptome analysis by RNA-seq.(A) The number of differentially expressed genes in *M. smegmatis* Δ*disA* and *M. smegmatis* Δ*pde* strains; (B)Volcano plot analysis showing differential expression profile of genes between *M. smegmatis* WT and *M. smegmatis* Δ*disA*(left) and *M. smegmatis* WT and *M. smegmatis* Δ*pde* (right). The redline indicates log2 fold change≥1 and adjusted p-value≤0.05. (C) The pie chart represents the functional classification and pathway enrichment analysis of differentially expressed genes in *M. smegmatis* Δ*disA* and *M. smegmatis* Δ*pde* strains and classified into 3 different categories: Biological process (BP), Molecular function (MF), Cellular component (CC) along with percentage abundance.

enrichment analysis of genes in 3 following categories: Biological process (BP), Molecular function (MF), Cellular component (CC), and KEGG Pathway using Cluster Profiler R software (Fig. 5C). Gene Ontology (GO) and pathway terms, with multiple test p-value ≤ 0.05 were considered significant in our analysis and illustrated in the Bubble plot (Figs. S8 and S9) where the size of the bubble is proportionate to the number of genes involved, different colors highlighted different categories of functional classifications. The orange baseline indicated the p-value threshold (Benjamini-Hochberg p-value 0.05). GO enrichment results revealed that in the case of *M. smegmatis* Δ*disA* strain, several ribosomal proteins and translational machinery genes were significantly downregulated, later we confirmed that the Δ*disA* strain was moderately sensitive to several antibiotics targeting bacterial translation (data not shown). Apart from that, the Arginine biosynthesis pathway and several universal stress proteins were differentially expressed in the null c-di-AMP background (Table 1), which needs further investigation. In the case of *M. smegmatis* Δ*pde,* several genes for integral membrane protein and inner membrane proteins are differentially expressed compared to WT possibly due to high c-di-AMP levels inside the cells. In addition to that, genes involved in extracellular pathways, plasma membrane and cell wall synthesis were found to be significantly altered with a huge fold change in expression (Table 2). A large number of genes representing structural components of the cell wall and membrane porins could justify the contrasting surface properties of the *M. smegmatis* Δ*pde* strain with *M. smegmatis* WT. Next, we shortlisted some candidate genes from importantly regulated pathways with significantly varied expression levels and correlated with the observed phenotype. The top two enriched KEGG pathways in *M. smegmatis* Δ*disA* strain with significant genes were illustrated as representative images, where up and down-regulated genes were shaded red and green respectively (Fig. S10).

4. Discussion

In our study, we have sought to understand the role of c-di-AMP in *M. smegmatis* by comparing diverse phenotypes in strains with altered c-di-AMP levels. Unlike other second messengers in *M. smegma*tis, c-di-AMP synthesis and degradation have been carried out by two different enzymes resulting in strict regulation of steady-state homeostasis, which is critical for normal cell growth and maintaining important physiological functions [45]. Since c-di-AMP is known to be dispensable in mycobacteria [14,44,46], it gave us an ideal opportunity to individually delete the genes responsible for the c-di-AMP synthesis and degradation to check the precise relevance of the molecule during normal growth and under relevant stress conditions (Fig. 6).

So far 5 major types of deadenylate cyclase (DAC) enzymes have been discovered, which are DacA, DisA, CdaA, CdaM, CdaS, and CdaZ [47]. Though the DisA class of DAC enzymes share the common N-terminal DAC domain with other more phylogenetically abundant classes like CdaA, in addition, it possesses a C-terminal DNA binding helix-hairpin-helix (HhH1) domain for monitoring DNA damage [2]. Since *M. smegmatis* is not known to form endospores and DisA is the sole c-di-AMP synthase, it was important to reveal other molecular functions regulated by c-di-AMP and DisA and understand how c-di-AMP synthesis and DNA damage response functions of the DisA enzyme in *M. smegmatis* get coordinated. First, we observed that the high c-di-AMP concentration affected several basic phenotypes like cell shape, cell length and cell width uniformity with visible differences in the strains' growth profile. The colony appearances changed drastically with increased c-di-AMP concentration related to altered cell surface properties, which is further corroborated by different cellular aggregation profiles and surface hydrophobicity in Δ*pde* strain. Further, we found that high c-di-AMP concentration does not favor the biofilm as well as air-liquid interphase pellicle formation. All these observations particularly for the Δ*pde* strain could be attributed to a major change in cell wall structure which was also pointed out by RNA-seq data. Next, we checked Δ*disA* and Δ*pde* mutants' survival patterns under different stresses and found that varying c-di-AMP concentration could play a definite role which is linked to underlying pathways yet to be discovered. The Δ*pde* mutant was found to be very sensitive to UV irradiation compared to WT, possibly due to the RecA enzyme's functional deficiency [11] and the Δ*disA* strain has better survival under identical conditions. Another genotoxic stress MMS treatment made Δ*disA* mutant extremely sensitive, which could possibly indicate the relevance of DNA scanning properties of the enzyme DisA, not the c-di-AMP synthesis. SDS treatment revealed that both

Table 1
Genes under several main categories are listed which are significantly downregulated in *M. smegmatis* Δ*disA* strain compared to *M. smegmatis* WT along with their function, log2fold change, and p-values.

Sl. No.	Component/Pathway/Function	Genes	Gene function	log2 fold change	p-value
1	Ribosome structure and function	rpsR2 (MSMEG_6895)	30S ribosomal protein S18	−2.05	0.048
2		rpmE (MSMEG_4951)	50S ribosomal protein L31	−1.73	0.034
3		rpmH (MSMEG_6946)	50S ribosomal protein L34	−1.13	0.031
4		rpsT (MSMEG_4571)	30S ribosomal protein S20	−1.60	0.023
5		rplL (MSMEG_1365)	50S ribosomal protein L7/L12	−2.43	0.027
6		rplI (MSMEG_6894)	50S ribosomal protein L9	−1.94	0.039
7		rpsP (MSMEG_2435)	30S ribosomal protein S16	−2.17	0.023
8		rpmG1 (MSMEG_1339)	50S ribosomal protein L33	−1.59	0.009
9		Pth (MSMEG_5432)	Peptidyl-tRNA hydrolase	−1.25	0.018
10	Response to stress	MSMEG_5733	Universal stress protein	−2.98	0.03
11		MSMEG_5245	Universal stress protein	−3.21	0.03
12		MSMEG_4207	Universal stress protein	−2.48	0.041
13		MSMEG_3950	Universal stress protein	−3.12	0.024
14	Arginine biosynthetic process	argF (MSMEG_3772)	Ornithine carbamoyltransferase	−1.12	0.033
15		argB (MSMEG_3774)	Acetylglutamate kinase	−1.17	0.025
16		argD (MSMEG_3773)	Acetylornithine aminotransferase	−1.25	0.049

Table 2
Genes under several main categories are listed which are significantly downregulated in *M. smegmatis* Δ*pde* strain compared to *M. smegmatis* WT along with their function, log2fold change, and p-values.

Sl. No.	Component/Pathway/Function	Genes	Gene function	log2 fold change	P-value
1	Extracellular region and cell wall	ripA (MSMEG_3145)	Peptidoglycan endopeptidase RipA	−1.49	0.037
2		mspA (MSMEG_0965)	Porin MspA	−2.00	0.042
3		mspB (MSMEG_0520	Porin MspB	−1.08	0.048
4	Sulfate transmembrane-transporting ATPase activity	cysT (MSMEG_4532)	Cysteine synthase B	−1.39	0.04
5		MSMEG_4533	Sulfate-binding protein	−1.35	0.044
6	Monosaccharide-transporting ATPase activity	MSMEG_6018	Xylose transport system permease	−1.39	0.038
7		MSMEG_4656	Sugar ABC transporter ATP-binding protein	−1.21	0.047
8	Plasma membrane	MSMEG_0549	ABC transporter, permease protein	−1.35	0.040
9		MSMEG_4657	ABC transporter membrane protein	−1.11	0.057
10		MSMEG_5060	ABC transporter, permease protein SugA	−1.51	0.0361
11		MSMEG_0642	Hypothetical ABC transporter permease protein YliD	1.32	0.044
12		MSMEG_0549	ABC transporter, permease protein	−1.35	0.040
13		MSMEG_6307	Glutamine-binding periplasmic protein/glutamine transport system permease protein	−1.49	0.036
14		MSMEG_1064	Phosphate transporter	−1.43	0.039
15		MSMEG_0140	Probable conserved mce associated membrane protein	−1.42	0.038
16		MSMEG_0142	Mammalian cell entry (mce) protein	−1.29	0.043
17		MSMEG_0143	Probable conserved mce associated membrane protein	−1.52	0.035
18		MSMEG_1144	Virulence factor Mce family protein	−1.22	0.040
19		MSMEG_1145	Virulence factor Mce family protein	−1.20	0.043
20		MSMEG_5895	Virulence factor Mce family protein	−1.25	0.045

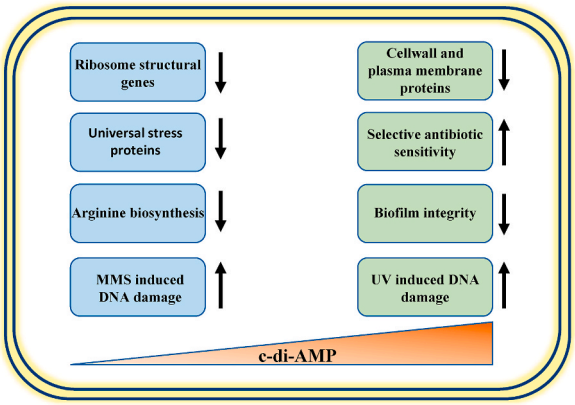

Fig. 6. Schematic representation showing different cellular pathways and phenotypes regulated by c-di-AMP concentration in *M. smegmatis*. The blue and green rectangles depict the c-di-AMP-null and c-di-AMP- overproduction phenotypes respectively. (For interpretation of the references to color in this figure legend, the reader is referred to the Web version of this article.)

high and no c-di-AMP inside cells could be detrimental for the bacteria as possibly related to RNA-seq data where several cell wall and integral membrane protein synthesis genes/pathways seemed to be under the direct control of c-di-AMP. Next, by putting precise point mutations in different domains of the DisA protein we could see that even if the one activity (c-di-AMP synthesis) of the enzyme is abolished, the other activity (DNA binding) remains unchanged, hence confirming the domain independency of DisA enzyme. Our Phenotypic Microarray analysis revealed how c-di-AMP concentration could play a major role in drug sensitivity by altering AUC values at specific antibiotic concentrations. In most of the cases, Δ*pde* mutant showed hypersensitivity to different antibiotic classes with the diverse mechanism of action (MOA) further corroborated by the difference in MIC and zone of inhibition (ZOE) studies. *M. smegmatis* Δ*pde* is sensitive against ciprofloxacin, rifampicin, erythromycin and vancomycin. Further studies are already underway to discover the underlying molecular mechanisms of drug sensitivity related to the c-di-AMP level. On all occasions, *M. smegmatis* Δ*disA* showed marginal resistance or no difference compared to WT implying the importance of maintaining optimum c-di-AMP concentrations inside cells. Previous studies have shown the direct link between increased c-di-AMP concentration with beta-lactam resistance in different gram-positive bacteria [4,5,48,49], although the mechanism was not well demonstrated. This effect only against cell

wall inhibitors could be justified by a specific class of DAC enzyme (other than DisA) and its operon structure, known to directly modulate cell wall biosynthesis and osmolyte transport. In our case we observed the opposite result that the Δ*pde* strain is sensitive to vancomycin compared to WT; which seemed more due to the downregulation of several genes in the cell wall and extracellular factors as evidenced by RNA-seq data. Precise information about the pathway and mechanisms remain to be discovered in the future. Other than that, in *Listeria monocytogenes,* deletion of c-di-AMP synthase enzymes are linked to beta-lactam sensitivity, which again had some relationship with the intracellular localization of the membrane protein [50,51]. In our case, Δ*disA* showed hardly any modulation in drug sensitivity against different classes of antibiotics implicating there was no similar mechanism involved in *M. smegmatis*. Rather, our data suggest that Δ*disA* is sensitive to aminoglycosides and marginally resistant to fluoroquinolone by diverse mechanisms (data not shown). Recently it was shown how the high c-di-AMP concentration mechanistically plays a role in antibiotic-resistant mutant generation in *M. smegmatis*, which again implicates the complex role of c-di-AMP messenger in the context of antibiotic resistance phenotypes in mycobacteria [52]. Finally, RNA-seq based transcriptome analysis revealed alternative gene expression profiles in null- and overproducing c-di-AMP mutants. Comparative analysis revealed 3-fold more genes were differentially expressed in Δ*disA* mutant compared to Δ*pde* mutant. Our analysis pointed out c-di-AMP driven regulation of several ribosomal structural genes which needs further investigation. Apart from that, several other pathways were shown to be affected in c-di-AMP null strain including efflux pump regulation, arginine biosynthesis and FAD binding. In the case of Δ*pde* mutant, several components of the cellwall and membrane biosynthesis were affected due to high c-di-AMP levels. Some of the key genes and pathways mainly related to antibiotic response, regulated by c-di-AMP which were first identified by phenotypic microarray, then correlated with RNA-seq analysis were further verified by us through other assays along with complementation constructs. Important mechanistic insights revealed that c-di-AMP acts as a crucial determinant for regulating drug susceptibility/resistance phenotypes in *M. smegmatis* (data not shown).

All in all, our study has revealed many novel phenotypes related to c-di-AMP in mycobacteria. Our ongoing and future research will bring out more interesting findings and hopefully further translate this crucial knowledge to understand *M. tuberculosis* physiology.

Author contribution statement

Vikas Chaudhary: conceived and designed the experiments; performed the experiments; analyzed and interpreted the data; contributed reagents, materials, analysis tools or data; wrote the paper.

Aditya Kumar Pal: designed and performed the experiments; analyzed and interpreted the data; contributed reagents, materials, analysis tools or data; wrote the paper.

Mamta Singla: performed the experiments; contributed reagents, materials, analysis tools or data.

Anirban Ghosh: conceived and designed the experiments; performed the experiments; analyzed and interpreted the data; contributed reagents, materials, analysis tools or data; wrote the paper.

Funding statement

This study was supported by the grant BT/RLF/Re-entry/31/2017 to Dr. Anirban Ghosh, by Department of Biotechnology (DBT), Government of India.

Data availability statement

Data will be made available on request.

Declaration of competing interest

The authors declare that they have no known competing financial interests or personal relationships that could have appeared to influence the work reported in this paper.

Acknowledgement

AG thanks the Department of Biotechnology (DBT), Government of India, for funding this work VC, AP, and MS acknowledge the Department of Biotechnology (DBT), Government of India for their fellowships. We acknowledge Ms Sunita Prakash, Indian Institute of Science, Bangalore for her help in sample analysis with MALDI-TOF mass spectrometry. We thank Dr. Sushma Krishnan, Indian Institute of Science, Bangalore and Dr. Preeti Bhardwaj, NCBS, Bangalore for performing TEM and SEM microscopy respectively. We thank Prof. Dipankar Chatterji, Indian Institute of Science, Bangalore for valuable feedback on the work.

Appendix A. Supplementary data

Supplementary data to this article can be found online at https://doi.org/10.1016/j.heliyon.2023.e15686.

References

[1] U. Römling, Great times for small molecules: c-di-AMP, a second messenger candidate in Bacteria and Archaea, Sci. Signal. 1 (2008), https://doi.org/10.1126/SCISIGNAL.133PE39.

[2] G. Witte, S. Hartung, K. Büttner, K.P. Hopfner, Structural biochemistry of a bacterial checkpoint protein reveals diadenylate cyclase activity regulated by DNA recombination intermediates, Mol. Cell 30 (2008) 167–178, https://doi.org/10.1016/J.MOLCEL.2008.02.020.

[3] Y. Oppenheimer-Shaanan, E. Wexselblatt, J. Katzhendler, E. Yavin, S. Ben-Yehuda, c-di-AMP reports DNA integrity during sporulation in Bacillus subtilis, EMBO Rep. 12 (2011) 594, https://doi.org/10.1038/EMBOR.2011.77.

[4] R.M. Corrigan, J.C. Abbott, H. Burhenne, V. Kaever, A. Gründling, c-di-AMP is a new second messenger in Staphylococcus aureus with a role in controlling cell size and envelope stress, PLoS Pathog. 7 (2011), e1002217, https://doi.org/10.1371/JOURNAL.PPAT.1002217.

[5] Y. Luo, J.D. Helmann, Analysis of the role of Bacillus subtilis σ(M) in β-lactam resistance reveals an essential role for c-di-AMP in peptidoglycan homeostasis, Mol. Microbiol. 83 (2012) 623–639, https://doi.org/10.1111/J.1365-2958.2011.07953.X.

[6] R.M. Corrigan, I. Campeotto, T. Jeganathan, K.G. Roelofs, V.T. Lee, A. Gründling, Systematic identification of conserved bacterial c-di-AMP receptor proteins, Proc. Natl. Acad. Sci. U. S. A. 110 (2013) 9084–9089, https://doi.org/10.1073/PNAS.1300595110/-/DCSUPPLEMENTAL.

[7] K. Sureka, P.H. Choi, M. Precit, M. Delince, D.A. Pensinger, T.A.N. Huynh, A.R. Jurado, Y.A. Goo, M. Sadilek, A.T. Iavarone, J.D. Sauer, L. Tong, J.J. Woodward, The cyclic dinucleotide c-di-AMP is an allosteric regulator of metabolic enzyme function, Cell 158 (2014) 1389–1401, https://doi.org/10.1016/J.CELL.2014.07.046.

[8] J.J. Woodward, A.T. Lavarone, D.A. Portnoy, c-di-AMP secreted by intracellular Listeria monocytogenes activates a host type I interferon response, Science 328 (2010) 1703–1705, https://doi.org/10.1126/SCIENCE.1189801.

[9] K. Parvatiyar, Z. Zhang, R.M. Teles, S. Ouyang, Y. Jiang, S.S. Iyer, S.A. Zaver, M. Schenk, S. Zeng, W. Zhong, Z.J. Liu, R.L. Modlin, Y.J. Liu, G. Cheng, The helicase DDX41 recognizes the bacterial secondary messengers cyclic di-GMP and cyclic di-AMP to activate a type I interferon immune response, Nat. Immunol. 13 (2012) 1155–1161, https://doi.org/10.1038/NI.2460.

[10] Q. Tang, Y. Luo, C. Zheng, K. Yin, M.K. Ali, X. Li, J. He, Functional analysis of a c-di-AMP-specific phosphodiesterase MsPDE from Mycobacterium smegmatis, Int. J. Biol. Sci. 11 (2015) 813–824, https://doi.org/10.7150/IJBS.11797.

[11] K. Manikandan, D. Prasad, A. Srivastava, N. Singh, S. Dabeer, A. Krishnan, K. Muniyappa, K.M. Sinha, The second messenger cyclic di-AMP negatively regulates the expression of Mycobacterium smegmatis recA and attenuates DNA strand exchange through binding to the C-terminal motif of mycobacterial RecA proteins, Mol. Microbiol. 109 (2018) 600–614, https://doi.org/10.1111/MMI.13991.

[12] L. Zhang, W. Li, Z.G. He, DarR, a TetR-like transcriptional factor, is a cyclic di-AMP-responsive repressor in Mycobacterium smegmatis, J. Biol. Chem. 288 (2013) 3085–3096, https://doi.org/10.1074/JBC.M112.428110.

[13] Y. Bai, J. Yang, X. Zhou, X. Ding, L.E. Eisele, G. Bai, Mycobacterium tuberculosis Rv3586 (DacA) is a diadenylate cyclase that converts ATP or ADP into c-di-AMP, PLoS One 7 (2012), e35206, https://doi.org/10.1371/JOURNAL.PONE.0035206.

[14] K. Manikandan, V. Sabareesh, N. Singh, K. Saigal, U. Mechold, K.M. Sinha, Two-step synthesis and hydrolysis of cyclic di-AMP in Mycobacterium tuberculosis, PLoS One 9 (2014), e86096, https://doi.org/10.1371/JOURNAL.PONE.0086096.

[15] J. Yang, Y. Bai, Y. Zhang, V.D. Gabrielle, L. Jin, G. Bai, Deletion of the cyclic di-AMP phosphodiesterase gene (cnpB) in Mycobacterium tuberculosis leads to reduced virulence in a mouse model of infection, Mol. Microbiol. 93 (2014) 65–79, https://doi.org/10.1111/MMI.12641.

[16] X. Lei, Q. Fan, T. Huang, H. Liu, G. Zhao, X. Ding, Efficient circular gene knockout system for Burkholderiales strain DSM 7029 and Mycobacterium smegmatis mc2 155, Acta Biochim. Biophys. Sin (Shanghai). 51 (2019) 697–706, https://doi.org/10.1093/ABBS/GMZ054.

[17] B.K. Bharati, R.K. Swetha, D. Chatterji, Identification and characterization of starvation induced msdgc-1 promoter involved in the c-di-GMP turnover, Gene 528 (2013) 99–108, https://doi.org/10.1016/J.GENE.2013.07.043.

[18] S. Krishnan, A. Petchiappan, A. Singh, A. Bhatt, D. Chatterji, R-loop induced stress response by second (p)ppGpp synthetase in Mycobacterium smegmatis: functional and domain interdependence, Mol. Microbiol. 102 (2016) 168–182, https://doi.org/10.1111/MMI.13453.

[19] J.M. Chen, G.J. German, D.C. Alexander, H. Ren, T. Tan, J. Liu, Roles of Lsr2 in colony morphology and biofilm formation of Mycobacterium smegmatis, J. Bacteriol. 188 (2006) 633–641, https://doi.org/10.1128/JB.188.2.633-641.2006.

[20] S. Ghosh, S.S. Indi, V. Nagaraja, Regulation of lipid biosynthesis, sliding motility, and Biofilm Formation by a membrane-anchored nucleoid-associated protein of Mycobacterium tuberculosis, J. Bacteriol. 195 (2013) 1769, https://doi.org/10.1128/JB.02081-12.

[21] J.L. Dahl, Electron microscopy analysis of Mycobacterium tuberculosis cell division, FEMS Microbiol. Lett. 240 (2004) 15–20, https://doi.org/10.1016/J.FEMSLE.2004.09.004.

[22] K.R. Gupta, S. Kasetty, D. Chatterji, Novel functions of (p)ppGpp and cyclic di-GMP in mycobacterial physiology revealed by phenotype microarray analysis of wild-type and isogenic strains of Mycobacterium smegmatis, Appl. Environ. Microbiol. 81 (2015) 2571, https://doi.org/10.1128/AEM.03999-14.

[23] A. Martínez, S. Torello, R. Kolter, Sliding motility in mycobacteria, J. Bacteriol. 181 (1999) 7331, https://doi.org/10.1128/JB.181.23.7331-7338.1999.

[24] C. Deshayes, F. Laval, H. Montrozier, M. Daffé, G. Etienne, J.M. Reyrat, A glycosyltransferase involved in biosynthesis of triglycosylated glycopeptidolipids in Mycobacterium smegmatis: impact on surface properties, J. Bacteriol. 187 (2005) 7283, https://doi.org/10.1128/JB.187.21.7283-7291.2005.

[25] X.Z. Li, L. Zhang, H. Nikaido, Efflux pump-mediated intrinsic drug resistance in Mycobacterium smegmatis, Antimicrob. Agents Chemother. 48 (2004) 2415, https://doi.org/10.1128/AAC.48.7.2415-2423.2004.

[26] P. Agrawal, R. Varada, S. Sah, S. Bhattacharyya, U. Varshney, Species-specific interactions of arr with RplK mediate stringent response in bacteria, J. Bacteriol. 200 (2018), https://doi.org/10.1128/JB.00722-17.

[27] D.C. Whiteford, J.J. Klingelhoets, M.H. Bambenek, J.L. Dahl, Deletion of the histone-like protein (Hlp) from Mycobacterium smegmatis results in increased sensitivity to UV exposure, freezing and isoniazid, Microbiology (Read.) (Reading) 157 (2011) 327–335, https://doi.org/10.1099/MIC.0.045518-0.

[28] J.C. Palomino, A. Martin, M. Camacho, H. Guerra, J. Swings, F. Portaels, Resazurin microtiter assay plate: simple and inexpensive method for detection of drug resistance in Mycobacterium tuberculosis, Antimicrob. Agents Chemother. 46 (2002) 2720–2722, https://doi.org/10.1128/AAC.46.8.2720-2722.2002.

[29] M. Rawat, M. Uppal, G. Newton, M. Steffek, R.C. Fahey, Y. Av-Gay, Targeted mutagenesis of the Mycobacterium smegmatis mca gene, encoding a mycothiol-dependent detoxification protein, J. Bacteriol. 186 (2004) 6050, https://doi.org/10.1128/JB.186.18.6050-6058.2004.

[30] J.D. Maarsingh, S. Yang, J.G. Park, S.E. Haydel, Comparative transcriptomics reveals PrrAB-mediated control of metabolic, respiration, energy-generating, and dormancy pathways in Mycobacterium smegmatis, BMC Genom. 20 (2019) 1–16, https://doi.org/10.1186/S12864-019-6105-3/FIGURES/7.

[31] L. Zhang, Z.G. He, Radiation-sensitive gene A (RadA) targets DisA, DNA integrity scanning protein A, to negatively affect cyclic di-AMP synthesis activity in Mycobacterium smegmatis, J. Biol. Chem. 288 (2013), 22426, https://doi.org/10.1074/JBC.M113.464883.

[32] K.R. Gupta, P. Baloni, S.S. Indi, D. Chatterji, Regulation of growth, cell shape, cell division, and gene expression by second messengers (p)ppGpp and cyclic di-GMP in Mycobacterium smegmatis, J. Bacteriol. 198 (2016) 1414, https://doi.org/10.1128/JB.00126-16.

[33] J. Recht, A. Martínez, S. Torello, R. Kolter, Genetic analysis of sliding motility in Mycobacterium smegmatis, J. Bacteriol. 182 (2000) 4348–4351, https://doi.org/10.1128/JB.182.15.4348-4351.2000.

[34] J.S. Schorey, L. Sweet, The mycobacterial glycopeptidolipids: structure, function, and their role in pathogenesis, Glycobiology 18 (2008) 832, https://doi.org/10.1093/GLYCOB/CWN076.

[35] C.M. Pule, S.L. Sampson, R.M. Warren, P.A. Black, P.D. van Helden, T.C. Victor, G.E. Louw, Efflux pump inhibitors: targeting mycobacterial efflux systems to enhance TB therapy, J. Antimicrob. Chemother. 71 (2016) 17–26, https://doi.org/10.1093/JAC/DKV316.

[36] S.M. Massa, A.D. Sharma, C. Siletti, Z. Tu, J.J. Godfrey, W.G. Gutheil, T.A.N. Huynh, c-di-AMP accumulation impairs muropeptide synthesis in Listeria monocytogenes, J. Bacteriol. 202 (2020), https://doi.org/10.1128/JB.00307-20.

[37] B.K. Bharati, I.M. Sharma, S. Kasetty, M. Kumar, R. Mukherjee, D. Chatterji, A full-length bifunctional protein involved in c-di-GMP turnover is required for long-term survival under nutrient starvation in Mycobacterium smegmatis, Microbiology (Read.) 158 (2012) 1415–1427, https://doi.org/10.1099/MIC.0.053892-0.

[38] C. Gándara, J.C. Alonso, DisA and c-di-AMP act at the intersection between DNA-damage response and stress homeostasis in exponentially growing Bacillus subtilis cells, DNA Repair (Amst) 27 (2015) 1–8, https://doi.org/10.1016/J.DNAREP.2014.12.007.
[39] R. Torres, E. Serrano, K. Tramm, J.C. Alonso, Bacillus subtilis RadA/Sms contributes to chromosomal transformation and DNA repair in concert with RecA and circumvents replicative stress in concert with DisA, DNA Repair (Amst) 77 (2019) 45–57, https://doi.org/10.1016/J.DNAREP.2019.03.002.
[40] M. Bejerano-Sagie, Y. Oppenheimer-Shaanan, I. Berlatzky, A. Rouvinski, M. Meyerovich, S. Ben-Yehuda, A checkpoint protein that scans the chromosome for damage at the start of sporulation in Bacillus subtilis, Cell 125 (2006) 679–690, https://doi.org/10.1016/J.CELL.2006.03.039.
[41] C. Gándara, D.K.C. de Lucena, R. Torres, E. Serrano, S. Altenburger, P.L. Graumann, J.C. Alonso, Activity and in vivo dynamics of Bacillus subtilis DisA are affected by RadA/Sms and by Holliday junction-processing proteins, DNA Repair (Amst) 55 (2017) 17–30, https://doi.org/10.1016/J.DNAREP.2017.05.002.
[42] Y. Bai, J. Yang, T.M. Zarrella, Y. Zhang, D.W. Metzger, G. Bai, Cyclic di-AMP impairs potassium uptake mediated by a cyclic di-AMP binding protein in Streptococcus pneumoniae, J. Bacteriol. 196 (2014) 614, https://doi.org/10.1128/JB.01041-13.
[43] A. Petchiappan, S.Y. Naik, D. Chatterji, RelZ-mediated stress response in Mycobacterium smegmatis: pGpp synthesis and its regulation, J. Bacteriol. 202 (2020), https://doi.org/10.1128/JB.00444-19.
[44] X. Li, H. Mei, F. Chen, Q. Tang, Z. Yu, X. Cao, B.T. Andongma, S.H. Chou, J. He, Transcriptome landscape of Mycobacterium smegmatis, Front. Microbiol. 8 (2017) 2505, https://doi.org/10.3389/FMICB.2017.02505/BIBTEX.
[45] F.M. Commichau, A. Dickmanns, J. Gundlach, R. Ficner, J. Stülke, A jack of all trades: the multiple roles of the unique essential second messenger cyclic di-AMP, Mol. Microbiol. 97 (2015) 189–204, https://doi.org/10.1111/MMI.13026.
[46] P.S. Manzanillo, M.U. Shiloh, D.A. Portnoy, J.S. Cox, Mycobacterium tuberculosis activates the DNA-dependent cytosolic surveillance pathway within macrophages, Cell Host Microbe 11 (2012) 469–480, https://doi.org/10.1016/J.CHOM.2012.03.007.
[47] W. Yin, X. Cai, H. Ma, L. Zhu, Y. Zhang, S.H. Chou, M.Y. Galperin, J. He, A decade of research on the second messenger c-di-AMP, FEMS Microbiol. Rev. 44 (2020) 701, https://doi.org/10.1093/FEMSRE/FUAA019.
[48] J.M. Griffiths, A.J. O'Neill, Loss of function of the GdpP protein leads to joint β-lactam/glycopeptide tolerance in Staphylococcus aureus, Antimicrob. Agents Chemother. 56 (2012) 579, https://doi.org/10.1128/AAC.05148-11.
[49] H.T. Pham, W. Shi, Y. Xiang, S.Y. Foo, M.R. Plan, P. Courtin, M.P. Chapot-Chartier, E.J. Smid, Z.X. Liang, E. Marcellin, M.S. Turner, Cyclic di-AMP oversight of counter-ion osmolyte pools impacts intrinsic cefuroxime resistance in lactococcus lactis, mBio 12 (2021), https://doi.org/10.1128/MBIO.00324-21.
[50] A.T. Whiteley, N.E. Garelis, B.N. Peterson, P.H. Choi, L. Tong, J.J. Woodward, D.A. Portnoy, c-di-AMP modulates Listeria monocytogenes central metabolism to regulate growth, antibiotic resistance and osmoregulation, Mol. Microbiol. 104 (2017) 212–233, https://doi.org/10.1111/MMI.13622.
[51] J. Rismondo, J. Gibhardt, J. Rosenberg, V. Kaever, S. Halbedel, F.M. Commichau, Phenotypes associated with the essential diadenylate cyclase CdaA and its potential regulator CdaR in the human pathogen Listeria monocytogenes, J. Bacteriol. 198 (2016) 416, https://doi.org/10.1128/JB.00845-15.
[52] A.K. Pal, A. Ghosh, c-di-AMP signaling plays important role in determining antibiotic tolerance phenotypes of Mycobacterium smegmatis, Sci. Rep. 12 (2022) 1–13, https://doi.org/10.1038/s41598-022-17051-z.